A Store-operated Calcium Channel in *Drosophila* S2 Cells

Andriy V. Yeromin,[1] Jack Roos,[2] Kenneth A. Stauderman,[2] and Michael D. Cahalan[1]

[1]Department of Physiology and Biophysics, University of California, Irvine, CA 92697
[2]Neurogenetics, Inc., La Jolla, CA 92037

ABSTRACT Using whole-cell recording in *Drosophila* S2 cells, we characterized a Ca^{2+}-selective current that is activated by depletion of intracellular Ca^{2+} stores. Passive store depletion with a Ca^{2+}-free pipette solution containing 12 mM BAPTA activated an inwardly rectifying Ca^{2+} current with a reversal potential >60 mV. Inward currents developed with a delay and reached a maximum of 20–50 pA at −110 mV. This current doubled in amplitude upon increasing external Ca^{2+} from 2 to 20 mM and was not affected by substitution of choline for Na^+. A pipette solution containing ~300 nM free Ca^{2+} and 10 mM EGTA prevented spontaneous activation, but Ca^{2+} current activated promptly upon application of ionomycin or thapsigargin, or during dialysis with IP_3. Isotonic substitution of 20 mM Ca^{2+} by test divalent cations revealed a selectivity sequence of $Ba^{2+} > Sr^{2+} > Ca^{2+} >> Mg^{2+}$. Ba^{2+} and Sr^{2+} currents inactivated within seconds of exposure to zero-Ca^{2+} solution at a holding potential of 10 mV. Inactivation of Ba^{2+} and Sr^{2+} currents showed recovery during strong hyperpolarizing pulses. Noise analysis provided an estimate of unitary conductance values in 20 mM Ca^{2+} and Ba^{2+} of 36 and 420 fS, respectively. Upon removal of all external divalent ions, a transient monovalent current exhibited strong selectivity for Na^+ over Cs^+. The Ca^{2+} current was completely and reversibly blocked by Gd^{3+}, with an IC_{50} value of ~50 nM, and was also blocked by 20 μM SKF 96365 and by 20 μM 2-APB. At concentrations between 5 and 14 μM, application of 2-APB increased the magnitude of Ca^{2+} currents. We conclude that S2 cells express store-operated Ca^{2+} channels with many of the same biophysical characteristics as CRAC channels in mammalian cells.

KEY WORDS: *Drosophila* • S2 cell • calcium channel • store-operated Ca^{2+} influx • CRAC channel

INTRODUCTION

Store-operated Ca^{2+} (SOC) channels are characterized functionally by their activation in the surface membrane upon depletion of Ca^{2+} from the endoplasmic reticulum. SOC channels can be activated physiologically after IP_3-induced release of Ca^{2+}. Several biophysically distinct store-operated Ca^{2+} channels that mediate capacitative calcium entry have been investigated by patch clamp experiments in a variety of cell types over the past 10–15 yr. SOC channels exhibit varying degrees of selectivity for Ca^{2+}, ranging from Ca^{2+}-permeable channels that carry significant Na^+ current to channels that exhibit a high degree of selectivity for Ca^{2+} ions. In T lymphocytes and mast cells, a highly selective type of SOC channel, termed the Ca^{2+} release–activated Ca^{2+} (CRAC) channel, opens when IP_3-sensitive Ca^{2+} stores are emptied. CRAC channels exhibit an inwardly rectifying I-V characteristic and a transient monovalent current upon withdrawal of external divalent cations. The physiological significance of these channels is highlighted by their requirement for normal T cell activation via the phosphatase calcineurin and their absence in severely immunocompromised patients (Feske et al., 2001; Lewis, 2001). Although CRAC channels have been characterized biophysically in patch-clamp experiments, their mechanism of activation and molecular identity remain uncertain.

The original transient receptor potential (TRP) gene was isolated from a *Drosophila* mutant that lacks a component of Ca^{2+} current in photoreceptor cells (Minke et al., 1975; Montell and Rubin, 1989; Hardie and Minke, 1992). This current, originally thought to be store operated, is now thought to be activated by metabolic products downstream from the breakdown of phosphatidylinositol bisphosphate by phospholipase C (Hardie and Minke, 1995; Minke and Cook, 2002; Minke and Agam, 2003). Several members of the mammalian TRP gene family have been proposed as molecular candidates for the CRAC channel and for other SOC channels (Montell et al., 2002; Montell, 2003; Prakriya and Lewis, 2003). The *Drosophila* S2 cell line is widely used as an expression system, but ion channels that are endogenous to these cells have not been investigated in detail. Yagodin et al. (1998) reported the presence of a Gd^{3+}-sensitive calcium influx evoked by thapsigargin in the variant S2-DM1 *Drosophila* cell

Address correspondence to Michael D. Cahalan, Department of Physiology and Biophysics, University of California, Irvine, CA 92697-4561. Fax: (949) 824-3143; email: mcahalan@uci.edu

Abbreviations used in this paper: CRAC, Ca^{2+} release–activated Ca^{2+}; SOC, store-operated Ca^{2+}; TRP, transient receptor potential.

J. Gen. Physiol. © The Rockefeller University Press • 0022-1295/2004/02/167/16 $8.00
Volume 123 February 2004 167–182
http://www.jgp.org/cgi/doi/10.1085/jgp.200308982

line stably expressing muscarinic receptors. Here, we present the first characterization of a native store-operated current in *Drosophila* S2 cells and compare its properties of activation, inactivation, ion selectivity, and block by pharmacological agents to functional features of mammalian CRAC channels. *Drosophila* S2 cells provide a suitable platform for continued molecular and functional characterization of CRAC channels.

MATERIALS AND METHODS

Cell Culture

Drosophila S2 cells (Invitrogen) were cultured in Schneider's *Drosophila* medium containing 10% FCS and 1% glutamine (pH 6.6) at room temperature in a CO_2-free incubator. The cells were passed once a week at density of 10^6/ml.

Measurement of Intracellular Free Calcium Concentration

Drosophila S2 cells, plated in 384-well plates at 15–20 × 10^5 cells/well, were loaded with 2 μM fluo-4/AM (Molecular Probes) in Schneider's S2 culture medium containing 2.5 mM probenecid for 1 h at 22°C. Cells were then washed and bathed in a Ca^{2+}-free buffer containing in mM: 120 NaCl, 5 KCl, 4 $MgCl_2$, 32.2 sucrose, 10 HEPES, 0.1 EGTA, 2.5 probenecid, pH 7.2 adjusted by NaOH. Fluorescence was monitored with a FLIPR^{384} (Molecular Devices) at room temperature. Initial fluorescence levels were recorded for 30 s, followed by addition of vehicle (0.01% DMSO) or 1 μM thapsigargin (LC Labs). 5 min later $CaCl_2$ (final concentration 1.8 mM) was added to each well and the response monitored for an additional 3 min.

Whole-cell Recording

Patch-clamp experiments were performed at room temperature in the standard whole-cell recording configuration (Hamill et al., 1981). Pipettes were pulled from soft glass capillaries (Disposable soda lime glass microhematocrit tubes; Kimble), coated with Sylgard (Dow Corning Corp.), and fire polished to a resistance of 2–3.5 MΩ when filled with internal solutions. Membrane currents were recorded using an EPC-9 patch-clamp amplifier (HEKA). Data were sampled at a rate of 5 kHz and digitally filtered at 0.5–2 kHz for analysis and display. Fast and slow capacitative transients were cancelled by the compensation circuitry of the EPC-9. The membrane capacitance of S2 cells selected for recording was 10.2 ± 0.5 pF (mean ± SEM, n = 100 cells). Membrane potentials were corrected for a liquid junction potential of −10 mV between the pipette and bath solutions. The series resistance (3–10 MΩ) was not compensated. The membrane potential was held at 10 mV, and 220-ms voltage ramps from −110 to +110 mV alternating with 220-ms pulses to −110 mV were delivered every 2 s. Up to eight I-V curves were averaged for display. Leak currents before channel activation were averaged (up to five sweeps) and subtracted from subsequent current records. Unless otherwise stated, leak-subtracted I-V curves are displayed. Longer duration pulses (660 ms) to −110 mV were applied in experiments to measure conductance fluctuations. Input resistances determined before store depletion were >10 GΩ. External solutions were changed by fast application using a gravity-driven perfusion system with output tip diameter of ~50 μm placed within ~50 μm from the cell. Six barrels were inserted near the output tip, and solution exchange controlled manually by valves. A complete local solution exchange was achieved within 2 s. Data were analyzed using Pulse (Heka Electronic), Origin (OriginLab Corp.), and Sigma Plot (RockWare, Inc.).

Solutions for Electrophysiology

Table I summarizes the external and internal solutions used for whole-cell recording. Solutions are referred to by number in the text; for example, many experiments on S2 cells were performed with external solution 1 and pipette solution 9. For measurement of relative permeabilities, Ca^{2+} was substituted by Mg^{2+}, Sr^{2+}, or Ba^{2+}. In some experiments, Na^+ in the external solution was replaced by choline or Cs^+. Divalent-free external solutions contained 10 mM HEDTA and zero divalent to reduce free Mg^{2+} and Ca^{2+} to <1 μM. Cs_4-BAPTA (Molecular Probes) or EGTA were added to buffer Ca^{2+}. For pharmacological evaluation, Gd^{3+}, SKF 96365, or 2-aminoethyldiphenyl borate (2-APB) were added to external solutions from appropriate water or DMSO stock solutions at a minimal dilution of 0.4%. IP_3, ionomycin (Calbiochem), and thapsigargin (Calbiochem) were used in experi-

TABLE I

Solutions for Whole-cell Recording

External	[Monovalent]	[Divalent]	[HEDTA]	[Cl^-]	[Sucrose]	
1	150 Na^+	2 Ca^{2+}	–	154	20	
2	150 choline	2 Ca^{2+}	–	154	25	
3	114 Na^+	20 Ca^{2+}	–	154	38	
4	114 Na^+	20 Mg^{2+}	–	154	38	
5	114 Na^+	20 Sr^{2+}	–	154	38	
6	114 Na^+	20 Ba^{2+}	–	154	38	
7	150 Na^+	–	10	150	–	
8	151 Cs^+	–	10	151	–	
Internal	**[Cs^+ aspartate]**	**[Ca^{2+}]**	**[Chelator]**	**Free [Ca^{2+}]**	**[Cl^-]**	**[Mg^{2+} gluconate]**
9	139	–	12 BAPTA	–	2	8
10	148	–	12 BAPTA	–	2	–
11	149	5.5	10 EGTA	310 nM	2	8

Unless noted, concentrations are in mM. Internal solutions contained 15 HEPES, titrated to pH 7.2 with CsOH. External solutions contained 10 HEPES, 10 glucose, and titrated to pH 6.6 with the appropriate hydroxide. The choline solution (2) was titrated with NaOH. Osmolalities were adjusted to within 1% of 325 mOsm/kg. Solution 9 was used for passive store depletion. Solution 11 was used to maintain Ca^{2+} within Ca^2 stores. Free $[Ca^{2+}]_i$ was calculated using Maxchelator (http://www.stanford.edu/~cpatton/maxc.html, C. Patton, Stanford University).

ments to evaluate the dependence on internal Ca^{2+} stores. Unless noted, chemicals were obtained from Sigma-Aldrich.

RESULTS

Capacitative Ca^{2+} Entry in S2 Cells

S2 cells have been reported to exhibit store-operated Ca^{2+} entry in response to carbachol stimulation when G-protein–coupled muscarinic receptors were expressed heterologously, or in response to treatment by ionomycin or thapsigargin to deplete intracellular Ca^{2+} stores (Yagodin et al., 1999; Cordova et al., 2003). Consistent with these studies, store-operated Ca^{2+} entry in S2 cells was detected using the fluorescent Ca^{2+} indicator fluo-4 in a multiwell fluorescence plate reader (Fig. 1). Thapsigargin (1 μM) added to a Ca^{2+}-free external solution first evoked a Ca^{2+}-release transient that was followed by a large and sustained Ca^{2+} signal upon readdition of extracellular Ca^{2+}. In the DMSO control run without thapsigargin, the Ca^{2+}-release transient was not observed, and Ca^{2+} readdition elicited a response smaller than that evoked by thapsigargin. Thapsigargin-stimulated Ca^{2+} entry in S2 cells can be inhibited by 100 μM Gd^{3+} (Yagodin et al., 1998). In our experiments, complete blockade of thapsigargin-dependent Ca^{2+} entry was achieved by addition of 1 μM Gd^{3+} (unpublished data). Together, the results above confirm the existence of a store-operated Ca^{2+} entry pathway in S2 cells and indicate that this pathway has sensitivity to Gd^{3+} similar to that exhibited by CRAC channels in mammalian cells (Ross and Cahalan, 1995). In further experiments described below, we characterized a Ca^{2+} current that likely underlies the store-operated Ca^{2+} entry response.

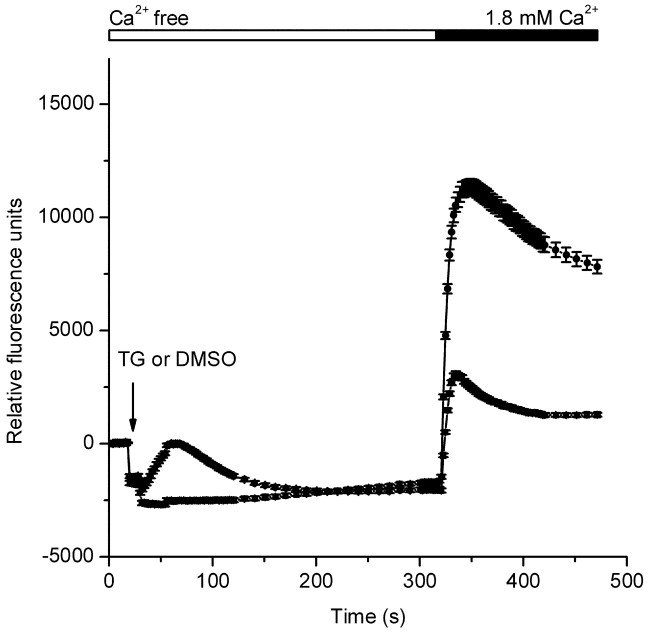

FIGURE 1. Thapsigargin-dependent Ca^{2+} entry in S2 cells. Fluo-4 fluorescence changes were monitored using a FLIPR^{384}. After 20 s of recording, the 384-well pipette-tip head was lowered into the solution creating an offset artifact in the recording. This offset artifact is unrelated to a cellular response and is dependent on the fluid volume in each well at the start of the experiment and the extent of tip penetration into the solution. 10 s after lowering the pipette-tip head, either thapsigargin (TG, 1 μM final, circles) or DMSO (triangles) was injected (arrow). $CaCl_2$ was then added to achieve a final concentration of 1.8 mM. Traces were zeroed at time 0, and each data point represents the mean (±SEM) of 192 replicates.

Ca^{2+} Current Induced by Dialysis with a Strong Ca^{2+} Buffer

A Ca^{2+}-selective current developed during prolonged dialysis of S2 cells with a Ca^{2+}-free pipette solution (9) containing 12 mM BAPTA, a pipette solution similar in composition to one that evokes passive depletion of Ca^{2+} stores and activation of CRAC channels in lymphocytes and mast cells. In Fig. 2 A, I-V curves during voltage ramps illustrate leak-subtracted currents after channel activation in 2 mM Ca^{2+}-containing external solution, and upon solution exchange to 20 mM Ca^{2+}. Current development, shown for a typical cell in Fig. 2 B, was characterized by an initial delay (t_d) that varied from 20 to 217 s, followed by an increase with a half-time of development ($t_{1/2}$) that varied from 17 to 163 s, leading to a steady level. Average parameters of activation are summarized in Table II. The peak current amplitude, evaluated at −110 mV with 2 mM external Ca^{2+}, of 35.6 ± 3.8 pA corresponds to an average current density of 3.3 ± 0.3 pA/pF (n = 64 cells). Upon increasing external [Ca^{2+}] to 20 mM, the current amplitude doubled at −110 mV (factor of 2.01 ± 0.04, n = 36). After reaching a peak, current amplitudes usually declined slowly. This process of "run-down" appeared to be faster in elevated extracellular Ca^{2+}. In 2 mM Ca^{2+}, 80% of current remained after 100 ± 11 s (n = 15), whereas in 20 mM Ca^{2+} the corresponding time was 53 ± 8 s (n = 28, $P < 0.001$). The current-voltage relationships (Fig. 2 A) in 2 and 20 mM external Ca^{2+} exhibited inward rectification, similar to I_{CRAC} in mammalian cells. Although varying external [Ca^{2+}] clearly altered the inward current magnitude, removal of Na^+ had no effect on either the current amplitude or the I-V shape (Fig. 2, C and D). The positive reversal potential of >60 mV indicates a P_{Ca}/P_{Cs} ratio of >2,000. From these experiments we conclude that a highly selective Ca^{2+} current, similar in I-V characteristics to mammalian CRAC current, develops under conditions that induce passive depletion of Ca^{2+}-stores. Other currents, such as outwardly rectifying Mg^{2+}-inhibited cation (MIC, also know as MagNuM) current ubiquitously present in mammalian cells (Hermosura et al., 2002; Kozak et al., 2002; Prakriya and Lewis, 2002) did not

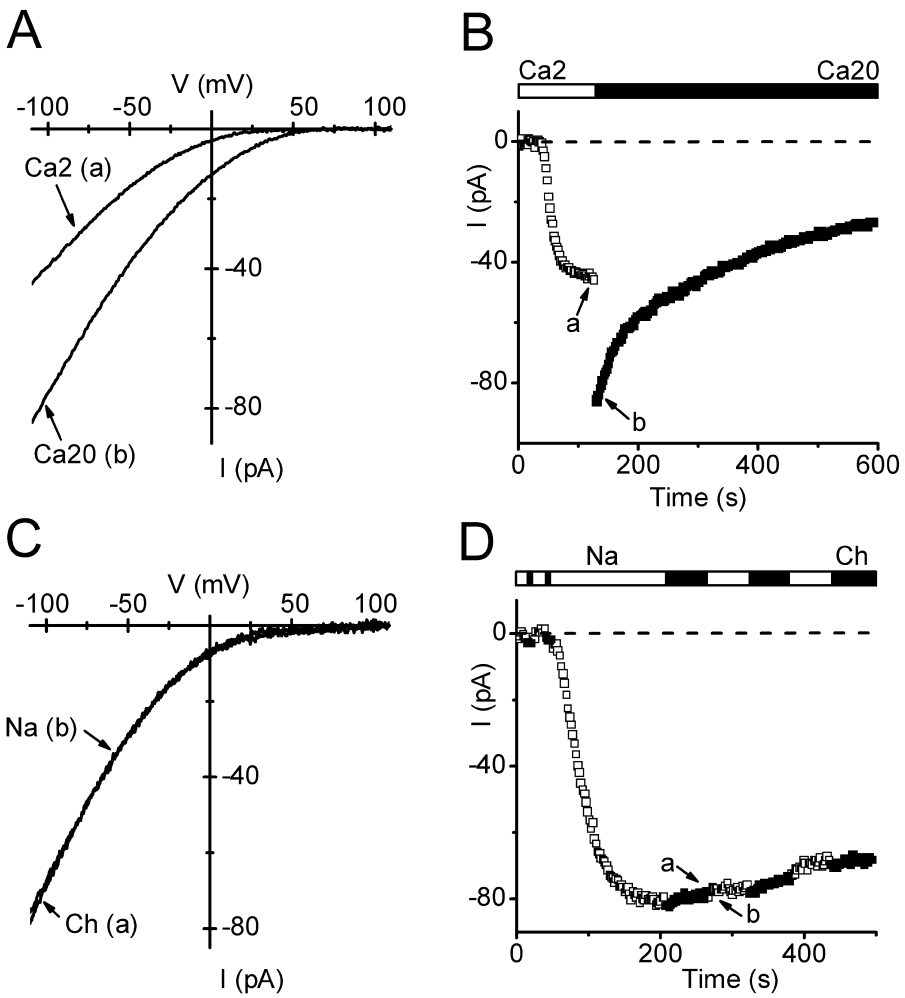

FIGURE 2. Development of inwardly rectifying Ca^{2+} current during dialysis with BAPTA. Pipette solution 9 (passive store depletion). (A) I-V relations during voltage ramps from −110 to +110 mV in external solutions containing 2 or 20 mM Ca^{2+}. (B) Time course of Ca^{2+} currents measured at −110 mV at varying times after break-in to achieve whole-cell recording. Open and solid bars above represent exposure to 2 (□) or 20 (■) mM Ca^{2+} (solutions 1 and 3). Arrows a and b indicate the time corresponding to I-V curves in A. (C) Leak-subtracted I-V relations of Ca^{2+} current in Na^+ or choline (Ch) external solutions (1 and 2). Leak traces were recorded in the presence of Na^+ or choline before current development. (D) Time course of Ca^{2+} current after break-in. Solid and open bars represent alternating exposure to Na^+ (□) and choline (Ch; ■). Arrows a and b indicate the time corresponding to I-V curves in C.

develop, even if internal Mg^{2+} was omitted (26 cells using solution 10, unpublished data).

Activation by Store Depletion

The distinguishing characteristic of a store-operated current is its activation in response to intracellular Ca^{2+} store depletion (Prakriya and Lewis, 2003). Accordingly, we investigated current development during procedures that prevent or actively cause store depletion. We anticipated that an EGTA-buffered pipette solution containing elevated free [Ca^{2+}] might promote Ca^{2+} retention in the stores, and consistent with expectation no current developed in 9 of 11 cells tested during 10 min of dialysis using solution 11 with 310 nM free $[Ca^{2+}]_i$ (Fig. 3 A); in the other two cells a tiny whole-cell current <2 pA was detected. When solutions with lower free $[Ca^{2+}]_i$ were evaluated, spontaneous activation of Ca^{2+} current occasionally occurred (unpublished data). These results set the stage for evaluating three agents known to induce active Ca^{2+}-store depletion: IP_3, thapsigargin, and ionomycin.

IP_3 opens IP_3-sensitive channels in the endoplasmic reticulum, leading to calcium influx as the Ca^{2+} store is depleted. When added to the pipette (10 μM in 13 cells and 5 μM in 9 cells, in solution 11), IP_3 induced a Ca^{2+} current in approximately half of the cells (combined data). Activation kinetics were highly variable. In 3 of 10 cells, current activated after a brief delay (<10 s) and then progressed rapidly with $t_{1/2}$ values <15 s, whereas in 7 cells current developed more slowly with activation delays averaging 120 s and $t_{1/2}$ values of 110 s. The inwardly rectifying I-V shapes were identical to that described above (unpublished data). In this condition, we would expect the store reuptake mechanism to be active and to permit refilling under conditions of increased Ca^{2+} influx. As shown in Fig. 3 B, the IP_3-induced Ca^{2+} current initially increased upon solution exchange to 20 mM external Ca^{2+}, but the current subsequently declined, suggesting that internal stores were refilling causing channels to close (deactivate). Returning to 2 mM Ca^{2+} initially reduced the current (by direct removal of the permeant ion), but later the current increased as channels reactivated. This process

TABLE II

Activation of Ca^{2+} Current

	Current density at −110 mV in 2 mM Ca^{2+}	Activation delay, t_d	Activation half-time, $t_{1/2}$	Number of cells in which current was detected
	pA/pF	*s*	*s*	
Passive store depletion	3.3 ± 0.3	75 ± 6	50 ± 3	63 of 68
Ca^{2+}-buffered control	0.14 ± 0.04	>600	>600	2 of 11
5 μM IP_3	2.1 ± 0.8	60 ± 28	60 ± 27	5 of 9
10 μM IP_3	2.0 ± 0.5	107 ± 36	97 ± 40	5 of 13
1 μM thapsigargin	1.9 ± 0.6	105 ± 41	99 ± 23	4 of 4
10 μM ionomycin	1.8 ± 0.4	20 ± 2	21 ± 1	4 of 4

Current density values are tabulated for cells that had detectable CRAC current. The limit of detection was ~0.5 pA.

could be repeated a few times before currents eventually declined. In summary, IP_3-induced depletion of the Ca^{2+} store activated a Ca^{2+} current that responded to elevated external Ca^{2+} in a manner consistent with store refilling.

Thapsigargin, a selective inhibitor of the SERCA pump, applied in the bath solution at 1 μM, also induced the Ca^{2+} current (in 4 out of 4 trials), with an average latency of ~100 s. Conventionally, activation of CRAC current by thapsigargin can be understood in

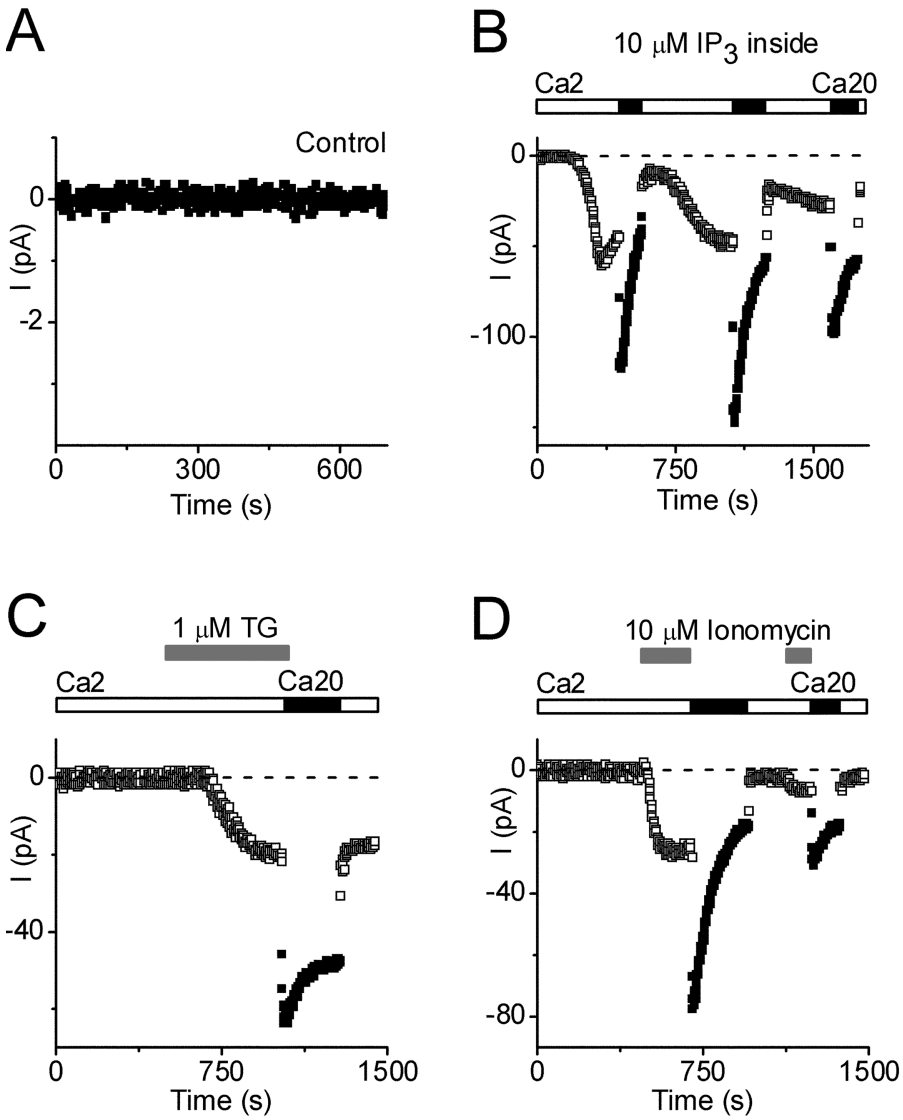

FIGURE 3. Activation of Ca^{2+} current by store depletion. Pipette solution 11 (Ca^{2+} buffered to 310 nM). (A) Control currents with no activation of Ca^{2+} current (note current scale). (B) IP_3-activated Ca^{2+} currents (10 μM IP_3 added to pipette), during exposure to 2 (□) or 20 (■) mM Ca^{2+}. Note complex changes in current during exposure to varying external Ca^{2+}. (C) Thapsigargin (TG, 1 μM) applied externally at indicated time (gray bars), during exposure to 2 (□) or 20 (■) mM Ca^{2+}. (D) Ionomycin (10 μM) applied externally at indicated times (gray bars), during exposure to 2 (□) or 20 (■) mM Ca^{2+}.

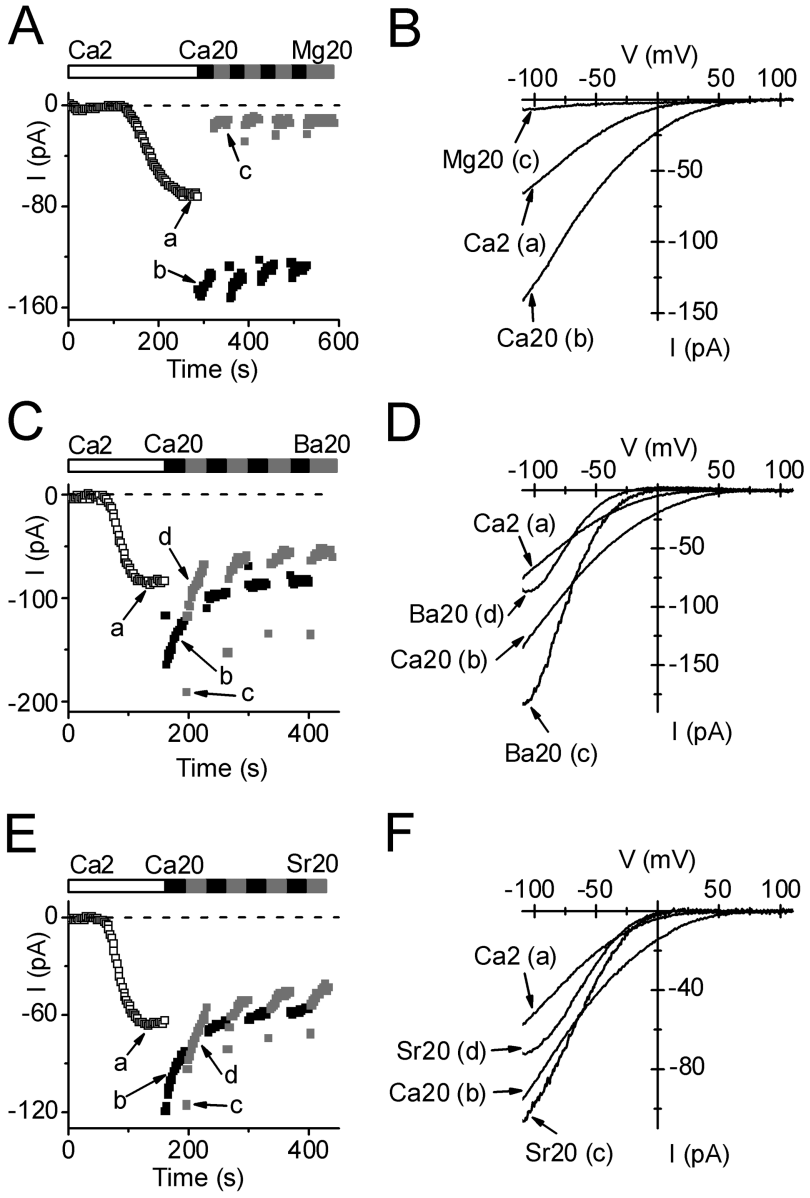

FIGURE 4. Selectivity among divalent cations. Pipette solution 9. Bars indicate exposure to varying divalent cations at indicated concentrations. Currents at −110 mV are shown during exposure to 2 (□) or 20 (■) mM Ca^{2+}, or to a test divalent cation (gray square). Labeled I-V curves were acquired at indicated times on corresponding development time courses. (A) Ion selectivity; $Ca^{2+} >> Mg^{2+}$. (B) I-V curves comparing 2 and 20 mM Ca^{2+} with 20 mM Mg^{2+}. (C) Ba^{2+} current. Note partial inactivation of current after changing to Ba^{2+}. (D) Ba^{2+} I-V relation; note "hook" and steeper inward rectification with Ba^{2+}. (E) Sr^{2+} current. Note partial inactivation of current after changing to Sr^{2+}. (F) Sr^{2+} I-V relation. Note steeper inward rectification with Sr^{2+}.

terms of a balance of pumping and leak across the endoplasmic reticulum that is tipped in favor of depletion by selective inhibition of the uptake pump. The current induced by external addition of thapsigargin was increased upon solution exchange to 20 mM Ca^{2+}, but the current did not decline as rapidly as with IP_3 (compare Fig. 3, B and C). The difference in kinetics between IP_3 and thapsigargin makes sense, since thapsigargin would inhibit the pump and prevent reuptake, thereby prolonging channel activity.

The third agent tested, ionomycin, is a membrane-permeable Ca^{2+} ionophore that rapidly activates CRAC channels in mammalian cells by promoting Ca^{2+} loss from the internal store. Bath addition of ionomycin (10 μM) rapidly activated a Ca^{2+} current with an average delay of 20 s (Fig. 3 D), consistent with its ability to release Ca^{2+} from the store. Activation by ionomycin was consistently more rapid than other methods of inducing CRAC current. After CRAC current was activated, increasing external Ca^{2+} to 20 mM (without ionomycin) caused an immediate increase in current followed by a decline, presumably as stores refilled. A second application of ionomycin subsequently reactivated CRAC current.

Table II summarizes the data on channel activation using a variety of conditions. We conclude that the Ca^{2+}-selective current in S2 cells can be activated by four independent means that have as their common property the ability to induce depletion of Ca^{2+} from intracellular stores.

Selectivity Among Divalent Ions

One hallmark of the CRAC channel in mammalian cells is its selectivity among various divalent cations, in-

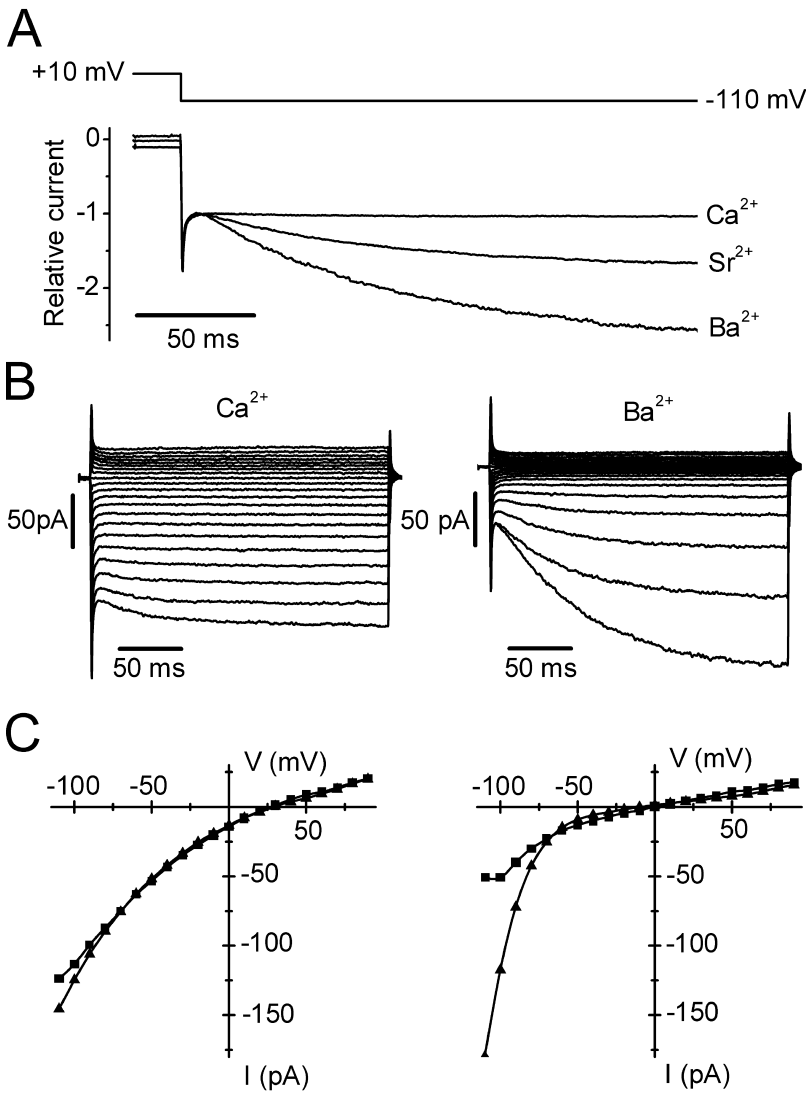

FIGURE 5. Ca^{2+}, Sr^{2+}, and Ba^{2+} currents during pulses. Pipette solution 9. (A) Comparison of normalized currents at −110 mV with 20 mM Ca^{2+}, Sr^{2+}, or Ba^{2+}. Note time-dependent increase in current with Sr^{2+} and Ba^{2+}. (B) Currents in response to voltage pulses ranging from −110 to +110 in 10-mV increments from the holding potential of 10 mV. Currents were recorded during exposure to 20 mM Ca^{2+} (left) or 20 mM Ba^{2+} (right). (C) Corresponding I-V curves (not leak subtracted) at beginning (squares) and end (triangles) of pulses. Note increased inward rectification at end of pulse with Ba^{2+}.

cluding the ability to carry Ba^{2+} and Sr^{2+}, but not Mg^{2+} (Parekh et al., 1997b; Prakriya and Lewis, 2003). To compare the divalent selectivity of store-operated channels in S2 cells, we waited for a steady level of current development, using passive store depletion (solution 9) to activate the channels, before applying external test divalent cations. As noted above and shown in Fig. 4 A, changing from 2 to 20 mM Ca^{2+} doubled the current amplitude, and then current began to decline. Subsequently, application of 20 mM Mg^{2+} greatly reduced, but did not completely eliminate, the inward current. I-V curves at three time points during this experiment are shown in Fig. 4 B. By changing to other divalent ions and measuring the initial current, we found the permeability sequence: $Ba^{2+} > Sr^{2+} > Ca^{2+} >> Mg^{2+}$.

With Sr^{2+} or Ba^{2+}, the time courses and I-V shapes revealed an additional complexity that likely represents a slow gating process revealed by removal of external Ca^{2+}. Immediately after changing from 20 mM Ca^{2+} to 20 mM Ba^{2+} or Sr^{2+}, the current initially increased but then declined rapidly with a time constant of <5 s to a new level (Fig. 4, C and E). We shall refer to this decline in Ba^{2+} (or Sr^{2+}) current as a form of channel inactivation. In a few experiments, we varied the mole fraction of Ca^{2+} and Ba^{2+} in order to determine whether inactivation was related to the absence of Ca^{2+} or the presence of Ba^{2+}. We found that 5 Ca^{2+}/15 Ba^{2+} behaved like 20 Ca^{2+} alone (unpublished data), i.e., current inactivation upon solution exchange was not observed, suggesting that inactivation was revealed when external Ca^{2+} was removed. Ramp I-V curves in Ba^{2+} or Sr^{2+} revealed changes in shape ("hooks", Fig. 4, D and F). To explore this phenomenon further, we used pulses instead of voltage ramps from the standard holding potential of +10 mV. At potentials more negative than −60 mV, we observed a time-dependent increase of Ba^{2+} or Sr^{2+} currents, as illustrated in Fig. 5 A. At −110 mV, Ba^{2+} and Sr^{2+} currents increased with

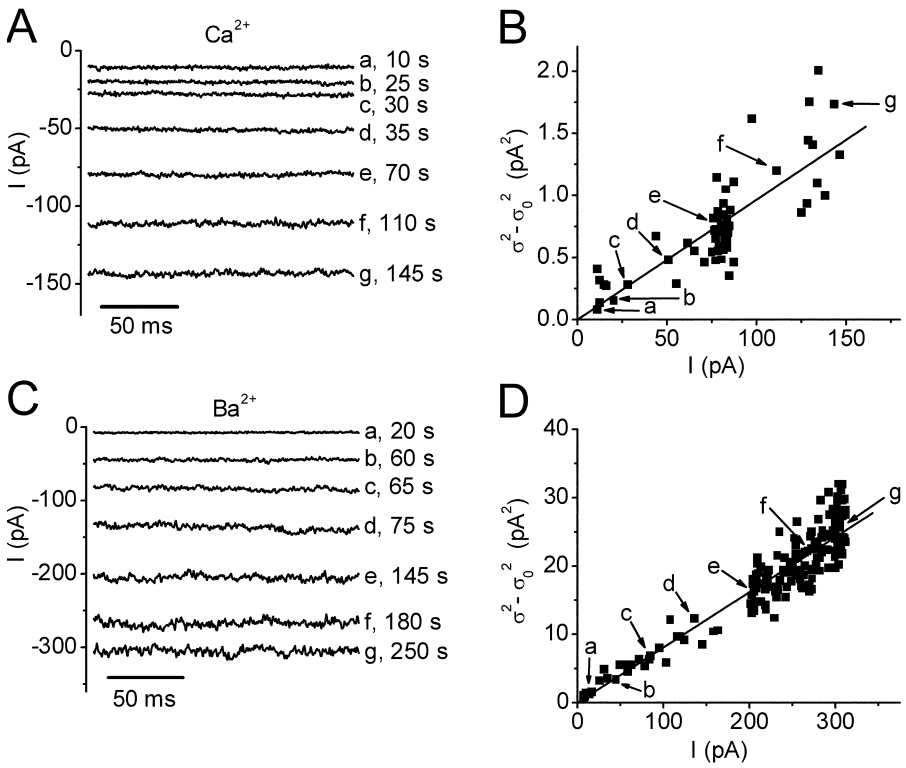

FIGURE 6. Noise analysis of divalent currents. Pipette solution 9. Currents at varying times, indicated to the right of each trace, in exemplary experiments with 20 mM Ca^{2+} (A) and 20 mM Ba^{2+} (C). Data were recorded at 5 kHz sampling and post-filtered at 1 kHz. Currents are shown during the last 180 ms of a 660 ms pulse to −110 mV. Ba^{2+} currents were corrected for ~3% residual activation by subtraction of a linear function. This procedure did not significantly affect the value of single-channel current. (B, D) Variance analysis of Ca^{2+} and Ba^{2+} currents. Background-subtracted variances ($\sigma^2 - \sigma_0^2$) plotted as a function of the mean current during the development of Ca^{2+} current (B) or Ba^{2+} current (D). Background variance was between 0.5 and 0.6 pA^2 in five experiments. The labeled points correspond to traces in A and C. Data are fitted by a linear function (n = 58, correlation coefficient 0.81 for Ca^{2+}; and n = 189, correlation coefficient 0.95 for Ba^{2+}). The slopes indicate a single channel current i of 9.7 ± 0.4 fA for Ca^{2+} and 80.8 ± 0.8 fA for Ba^{2+}.

time constants of ~90 ms for Ba^{2+} and ~80 ms for Sr^{2+}, leading to current potentiation after 220 ms by an average factor of 3.0 for Ba^{2+} and 1.5 for Sr^{2+}. To be certain that the potentiated Ba^{2+} current represents activity of the same Ca^{2+} channel, we checked two inhibitors described below and found that currents at the beginning and the end of hyperpolarizing pulses were affected equally by Gd^{3+} and by 2-APB. We also verified that Jurkat CRAC currents did not exhibit this time- and voltage-dependent component of Ba^{2+} current, consistent with previous observations (Zweifach and Lewis, 1995a). A complete set of S2 cell currents during varying voltage steps for Ca^{2+} and Ba^{2+} is shown in Fig. 5 B. Potentiation of the Ba^{2+} current leads to enhanced inward rectification measured at the end of the pulse, compared with the beginning (Fig. 5 C, right). Voltage-dependent potentiation of current at negative potentials was not observed in mixed Ca^{2+}/Ba^{2+} solutions; current did not increase during the hyperpolarizing pulse to −110 mV in a solution containing 5 mM Ca^{2+} and 15 mM Ba^{2+} (unpublished data). It is possible that hyperpolarizing pulses may reverse the inactivation of Ba^{2+} current observed upon solution exchange (see Fig. 4 C), since both exhibit the same mole-fraction dependence and both are capable of modulating the current magnitude to a similar extent. Regardless of mechanism, it is clear that Ba^{2+} (or Sr^{2+}) can carry significantly larger currents than Ca^{2+} in S2 cells.

Single-channel Current

To provide an estimate for the single-channel current carried by Ca^{2+} and Ba^{2+}, we analyzed conductance fluctuations during current development. Whole-cell currents were recorded in response to long-duration steps to −110 mV applied every 2 s, and variances and mean currents were computed during the last segment of each trace. Fig. 6 A illustrates the increase in mean Ca^{2+} current and noise during current development at varying times. Assuming that single-channel conductance remains constant and that current development corresponds to an increase in the open probability, a parabolic relationship between variance and mean current is predicted:

$$\sigma^2 - \sigma_0^2 = \bar{I}i(1 - P_o),$$

where $\bar{I}$ is the mean current, i the single-channel current, P_o the open probability, σ^2 the total variance, and σ_0^2 the background variance before current development. These assumptions are subject to the caveat that channel activation may not arise from an increase in P_o, but from an increase in the number of conducting channels. Using 1 kHz filtering, the background current variance determined before development of the current was 0.6 ± 0.2 pA^2 (n = 5). During current development, σ^2 grew in direct proportion to the mean current $\bar{I}$ (Fig. 6 B), possibly implying that P_o remained low throughout the experiment. From the

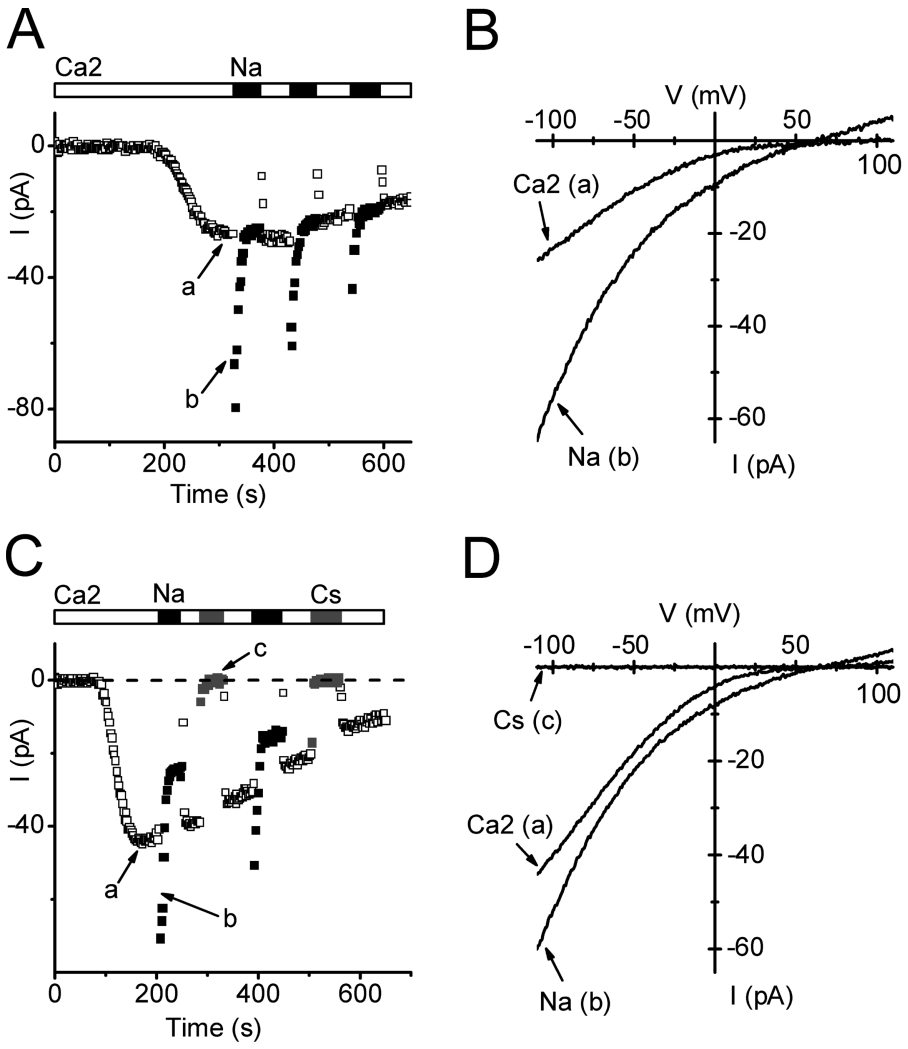

FIGURE 7. Store-operated current carried by Na^+ in divalent-free solution. Pipette solution 9. (A) Time course of currents after development of Ca^{2+} current with 2 mM external Ca^{2+} (□), and during subsequent exposure to divalent-free Na^+-containing solution (■; solution 7). (B) Corresponding Ca^{2+} and Na^+ I-V curves. (C) Cs^+ does not carry measurable monovalent current. After development of Ca^{2+} current (□), transient inward currents upon divalent withdrawal were only seen with Na^+ (■; solution 7) but not Cs^+ (gray square, solution 8). (D) Corresponding I-V curves.

slope of linear fits, we obtained an estimated single-channel current i in 20 mM Ca^{2+} that varied from 3.2 to 9.7 fA in five experiments, with an average of 6.9 ± 1.0 fA. Mean currents and variances were substantially larger with Ba^{2+} than with Ca^{2+}. After break-in to achieve whole-cell recording, mean Ba^{2+} currents increased along with increasing current noise (Fig. 6 C). During current development in 20 mM Ba^{2+}, a linear relationship between the current variance and mean currents was again obtained. From the slope of the background-subtracted $\sigma^2/\bar{I}$ relationship, the estimated single-channel current in 20 mM Ba^{2+} varied from 76 to 82 fA and averaged 80 ± 1 fA (n = 5). Changing the post-filtering from 1 to 2 kHz did not significantly affect these estimates, indicating that most of the channel noise power was below 1 kHz. Attempts to fit the variance/mean plots for both Ca^{2+} and Ba^{2+} failed if we supposed that P_o was > 0.1. Assuming a reversal potential of 80 mV, these estimated unitary currents correspond to a single-channel conductance of 420 fS with 20 mM Ba^{2+}, and 36 fS for 20 mM Ca^{2+}.

Permeability to Na^+ in Divalent-free External Solution

A further characteristic of many Ca^{2+} channels is the ability to carry monovalent ions upon complete withdrawal of divalent cations. For CRAC channels in mammalian cells, the monovalent current is transient, inactivating over a time course of tens of seconds, and Na^+, Li^+, K^+, Rb^+ are readily permeant, although Cs^+ permeability is much lower (Lepple-Wienhues and Cahalan, 1996). In contrast, the Ca^{2+}-permeable MIC channel in mammalian cells is less selective, allowing Cs^+ to permeate as well as Na^+ (Kozak et al., 2002; Prakriya and Lewis, 2002). In S2 cells, rapid exchange to divalent-free external solution (solution 7) exposed a transient Na^+ current that retained an inwardly rectifying characteristic, as shown in Fig. 7, A and B. The reversal potential of 62 mV implies a small outward Cs^+ current and a permeability ratio P_{Cs}/P_{Na} of 0.08. The Na^+ current was ~2 times larger than the immediately preceding Ca^{2+} current and then declined with a time constant of ~6 s to a new steady level. Upon readdition

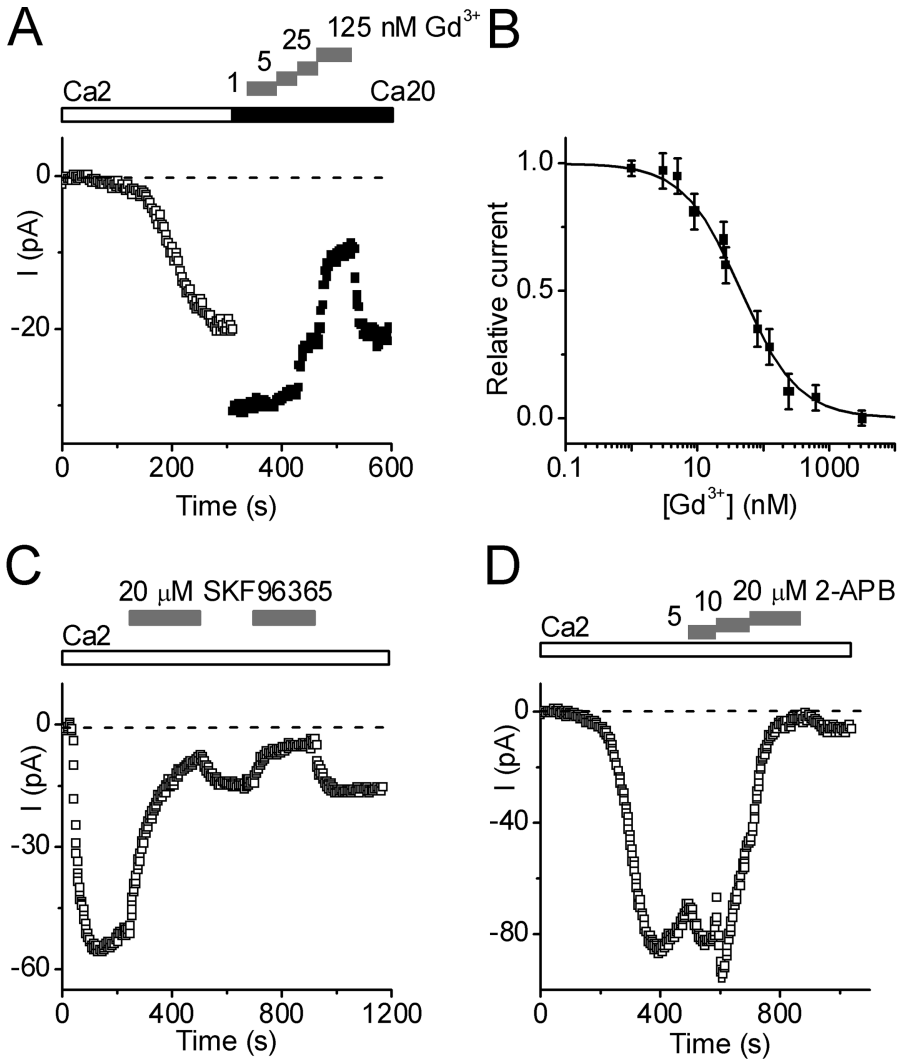

FIGURE 8. Pharmacological sensitivity to Gd^{3+}, SKF 96365, and 2-APB. Pipette solution 9. (A) Gd^{3+} block. After exposure to 2 Ca^{2+} (□), Gd^{3+} added to 20 mM Ca^{2+}-containing external solution (■) at progressively higher concentrations (gray bars) caused reversible block of Ca^{2+} current. (B) Dose-response curve for Gd^{3+} fitted to: $I/I_0 = IC_{50}/(IC_{50} + [Gd^{3+}])$, with IC_{50} value of 46 nM; combined data for 12 cells. (C) Effect of SKF 96365 (20 μM) on Ca^{2+} current. (D) Effect of 2-APB at indicated concentrations on Ca^{2+} current.

of 2 mM Ca^{2+}, current initially dropped but then recovered to the original steady level within 6 s. Cs^+ did not carry significant inward current during exposure to divalent-free external solution (Fig. 7, C and D). These features of monovalent current inactivation, potentiation by Ca^{2+}, and lack of Cs^+ current are qualitatively similar to those observed in mammalian CRAC channels (Christian et al., 1996; Lepple-Wienhues and Cahalan, 1996; Zweifach and Lewis, 1996).

Pharmacology

CRAC channels in mammalian cells are blocked by trivalent metal cations such as Gd^{3+} and La^{3+}, by SKF 96365, and can be increased or blocked by 2-APB depending upon the concentration. We tested these agents on the Ca^{2+} current in S2 cells.

Gd^{3+} reversibly blocked the Ca^{2+} current at nanomolar concentrations. Fig. 8 A shows the development of Ca^{2+} current in 2 mM Ca^{2+}. Replacement of the external solution by 20 mM Ca^{2+} caused an immediate increase in the current magnitude. Subsequently, addition of increasing concentrations of Gd^{3+} produced a graded inhibition of current. Block by Gd^{3+} was readily reversible. Fig. 8 B illustrates a dose–response curve with an IC_{50} value of 46 ± 3 nM (n = 12). Lanthanum (1 μM) also blocked this current completely (unpublished data). In contrast, block by SKF 96365 (20 mM) was slow to develop and did not reverse completely (Fig. 8 C). During the initial application, SKF inhibited the current progressively, and nearly complete inhibition was achieved within 250 s. Upon washout, the current recovery was only 20%. A second SKF 96365 application again blocked the current, and upon washout the current recovered to the same extent. Since the SKF 96365 effect was relatively slow and comparable with run-down, we did not estimate an IC_{50} value. In eight separate experiments, similar effects of SKF 96365 (5–20 mM) were observed. Effects of 2-APB on Ca^{2+} currents were more complex and exhibited both potentiation and inhibition in a concentration-

TABLE III

Comparison of CRAC Channels

Property	*Drosophila* CRAC	Mammalian CRAC	*C. elegans* SOC
Activation:			
By passive depletion	yes	yes	yes
By IP_3	yes	yes	yes
By thapsigargin	yes	yes	–
By ionomycin	yes	yes	yes
Inactivation:			
By store refilling	yes	yes	–
By local $[Ca^{2+}]_i$	no	yes, fast	no
Run-down	yes, ↑ by high Ca^{2+}	yes, ↑ by high Ca^{2+}	slow
In 0 Ca^{2+}/20 Ba^{2+}	yes, $\tau \sim 5$ s	yes, $\tau = 4$ s	no
Monovalent current	yes, $\tau \sim 6$ s	yes, $\tau \sim 10$ s	yes, $\tau > 100$ s
Divalent Selectivity:			
P_{Ca}/P_{Cs}	>2,000	>1,000	>1,000
Conductance sequence	$Ba^{2+} > Sr^{2+} > Ca^{2+} >> Mg^{2+}$ initially, then $Ca^{2+} > Sr^{2+} > Ba^{2+} >> Mg^{2+}$	$Ca^{2+} > Ba^{2+} \sim Sr^{2+} >> Mg^{2+}$	$Ca^{2+} > Ba^{2+} \sim Sr^{2+}$
γ (20 mM Ca^{2+})	36 fS	21 fS	–
Monovalent Selectivity:			
P_{Cs}/P_{Na}	0.08	0.09–0.13	0.6
Conductance sequence	$Na^+ >> Cs^+$	$Na^+ >> Cs^+$	$Na^+ >> Cs^+$
Pharmacology:			
Gd^{3+} or La^{3+}	nM (Gd^{3+}), reversible	nM (Gd^{3+}), reversible	mM (La^{3+}), reversible
SKF 96365	μM, partially reversible	μM, partially reversible	High μM, reversible
2-APB	Low μM, potentiation High μM, inhibition	Low μM, potentiation High μM, inhibition	Low μM, no effect High μM, inhibition

See text for full discussion and references. τ indicates time constant of exponential fit to indicated process. γ is the single-channel conductance estimated from measurement of variance and mean currents.

dependent manner, similar to that described previously in mammalian CRAC channels (Prakriya and Lewis, 2001). As shown in Fig. 8 D, application of 2-APB at a low concentration (5 mM) caused an increase in the current amplitude that opposed the rundown of current. Subsequently, increasing the 2-APB concentration to 10 μM further increased the current transiently, but then current began to fall. At higher concentrations (20 μM), 2-APB blocked the current, and little recovery was observed after drug washout. As with SKF 96365, block at high concentration was difficult to distinguish from accelerated rundown. In all cells tested, potentiation was consistently observed at concentrations between 5 and 14 μM ($n = 12$).

DISCUSSION

The S2 cell line was originally derived from a primary culture of late stage (20–24 h old) *Drosophila melanogaster* embryos and, based upon gene expression patterns and phagocytic activity, is thought to represent a haemocyte or macrophage-like cell (Schneider, 1972; Ramet et al., 2002). Previous reports have demonstrated the utility of S2 cells for studying Ca^{2+} signaling mechanisms (Hardie and Raghu, 1998; Yagodin et al., 1998, 1999; Swatton et al., 2001; Towers and Sattelle, 2002; Cordova et al., 2003). In this investigation, we confirmed the presence of a store-operated Ca^{2+} entry pathway in S2 cells, and then characterized the underlying store-operated Ca^{2+} current. We will refer to the ion channels that conduct this Ca^{2+} current as *Drosophila* CRAC channels because of the many similarities to "I_{CRAC}" in mammalian cells of hematopoietic origin (Hoth and Penner, 1993; Parekh and Penner, 1997; Prakriya and Lewis, 2003). Table III summarizes the properties of *Drosophila* and mammalian CRAC currents, alongside those of a SOC current described recently in *C. elegans* intestinal epithelial cells (Estevez et al., 2003). *Drosophila* and mammalian CRAC channels exhibit striking similarities in activation, ion permeation, and pharmacological sensitivity, differing primarily in inactivation properties that might be extrinsic to the channel protein. Moreover, CRAC current in S2 cells is not contaminated by other currents, and is present at high density in a cell line that provides distinct advantages for molecular characterization. Below we discuss these comparisons in greater detail.

Activation by Ca^{2+}-store Depletion

CRAC current was activated in S2 cells by four independent procedures that deplete intracellular Ca^{2+} stores. Dialysis with a pipette solution containing the Ca^{2+} chelator BAPTA (12 mM, solution 9) induced passive store depletion and activated *Drosophila* CRAC channels within 100 s (Fig. 2), similar to the time course for activation of mammalian CRAC channels by passive store depletion in Jurkat T cells (Lewis and Cahalan, 1989; Zweifach and Lewis, 1993; Ehring et al., 2000), rat mast cells (Hoth and Penner, 1993), RBL cells (Fasolato et al., 1993; Kozak et al., 2002), and also similar to SOC current in *C. elegans* intestinal epithelial cells (Estevez et al., 2003). IP_3 (5–10 μM) added to a control pipette solution that contained 310 nM free [Ca^{2+}] (solution 11) opened *Drosophila* CRAC channels in ~50% of tested cells with variable latencies. In mammalian cells (Hoth and Penner, 1992, 1993; Parekh et al., 1997a; Ehring et al., 2000; Bakowski and Parekh, 2002), as well as in *C. elegans* epithelial cells (Estevez et al., 2003), IP_3 added to highly buffered low Ca^{2+} pipette solutions consistently accelerated activation of CRAC or SOC current. However, with free $[Ca^{2+}]_i$ buffered to 90 nM, IP_3 activated CRAC current in an all-or-none fashion (Parekh et al., 1997a), consistent with our observation that IP_3 induced full CRAC channel activity in ~50% of cells. IP_3 alone is not always sufficient to activate CRAC current; added to a weak Ca^{2+} buffer it failed to activate CRAC currents unless thapsigargin was also added (Fierro and Parekh, 2000), a result that can be explained by reuptake of Ca^{2+} keeping stores filled adequately despite the activation of IP_3 receptors. Extracellular application of thapsigargin or the Ca^{2+} ionophore ionomycin also activated *Drosophila* CRAC channels, under conditions where the internal solution (control) was designed to favor Ca^{2+} retention in the stores (Fig. 3). These drugs and other SERCA pump inhibitors had similar effects in mammalian cells (Hoth and Penner, 1992; Zweifach and Lewis, 1993; Premack et al., 1994).

Deactivation and Inactivation

Once activated, CRAC channels are subject to modulation by refilling of intracellular Ca^{2+} stores and by additional consequences of elevated $[Ca^{2+}]_i$. Under conditions that permit active Ca^{2+}-store reuptake, deactivation of CRAC channels mediated by store refilling can explain the complex kinetics of CRAC currents in response to elevation of extracellular Ca^{2+} in experiments with IP_3 and ionomycin (Fig. 3), similar to previous studies in Jurkat cells (Zweifach and Lewis, 1995b). In contrast to deactivation, fast inactivation of mammalian CRAC current has been described as a local feedback mechanism that is sensed within a few nm of the channel and acts to close the channel rapidly in response to Ca^{2+} influx (Zweifach and Lewis, 1995a). This process appears to be absent in *Drosophila* CRAC channels, since currents are maintained during hyperpolarizing pulses (Fig. 5). Mammalian CRAC channels also appear to have a slow Ca^{2+}-dependent inactivation process that may contribute to run-down during maintained dialysis (Zweifach and Lewis, 1995b). Run-down of *Drosophila* CRAC channels was also enhanced by elevated external Ca^{2+}.

In both *Drosophila* and mammalian cells, complete removal of all divalent ions results in a monovalent current through CRAC channels that inactivates with similar kinetics (inactivation time constant of ~6 s for *Drosophila* CRAC channels, see Fig. 7, vs. ~10 s for mammalian CRAC channels; Lepple-Wienhues and Cahalan, 1996) much more quickly than *C. elegans* monovalent SOC current that inactivates at a rate of ~13%/min (Estevez et al., 2003). Inactivation of Ba^{2+} current appears to require both removal of Ca^{2+} and a depolarized potential; we used a holding potential of 10 mV during routine measurement of current development. Both inactivation and hyperpolarization-induced potentiation (Fig. 5 A) depended on removal of external Ca^{2+}, were not seen in mixed Ca^{2+}/Ba^{2+} external solutions, and progressed to a greater extent in Ba^{2+} than in Sr^{2+}. Upon withdrawal of external Ca^{2+}, Ba^{2+} current inactivation (Fig. 4 C) proceeded with a similar time course to Na^+ current inactivation induced by complete withdrawal of divalent ions (Fig. 7 A), and recovery of Ca^{2+} current upon readdition of external Ca^{2+} was fast (<10 s) in both cases. Monovalent Na^+ current inactivation has been described previously as a removal of the potentiating effect of extracellular Ca^{2+} (Christian et al., 1996; Lepple-Wienhues and Cahalan, 1996; Zweifach and Lewis, 1996). Further experiments will be needed to determine the possible relationship between inactivation of Ba^{2+} current and inactivation of monovalent current during divalent withdrawal. In summary, the *Drosophila* CRAC channel, like the mammalian CRAC channel, exhibits deactivation upon store refilling, Ca^{2+}-dependent rundown, inactivation of monovalent current upon removal of external divalents, and Ca^{2+}-dependent potentiation, but lacks fast inactivation mediated locally by Ca^{2+} influx.

Ion Selectivity

CRAC channels, both mammalian and in *Drosophila*, exhibit a very high degree of selectivity for Ca^{2+} over monovalent cations in physiological salt solutions. Based upon a reversal potential of >60 mV, the permeability ratio P_{Ca}/P_{Cs} is >2,000 (Fig. 2). Furthermore, in the presence of external Ca^{2+} ions, choline substitution provided no evidence for a component of inward Na^+ current, implying that Na^+ permeability in the presence of external Ca^{2+} is negligible. The divalent con-

ductance sequence for *Drosophila* CRAC channels depends on the measurement conditions. Immediately after solution exchange, Ba^{2+} was clearly the most permeant among the four divalent cations tested, in a conductance sequence $Ba^{2+} > Sr^{2+} > Ca^{2+} >> Mg^{2+}$. However, Ba^{2+} and Sr^{2+} currents inactivated rapidly, leading to a steady-state conductance sequence of $Ca^{2+} > Sr^{2+} > Ba^{2+} >> Mg^{2+}$. In mammalian cells, CRAC currents are usually larger with Ca^{2+} than Ba^{2+} or Sr^{2+} (Hoth and Penner, 1993; Zweifach and Lewis, 1993; Fierro and Parekh, 2000), although the sequence may depend upon the cell type (Hoth, 1995) or the measurement conditions since Ba^{2+} does not support Ca^{2+}-dependent potentiation (Christian et al., 1996).

Like voltage-activated Ca^{2+} channels (Almers and McCleskey, 1984; Hess and Tsien, 1984), CRAC channels are permeable to monovalent ions when divalent ions are removed (Hoth and Penner, 1993; Lepple-Wienhues and Cahalan, 1996). It is well established that mammalian CRAC channels conduct Na^+ much better than Cs^+ in the absence of divalent ions (Lepple-Wienhues and Cahalan, 1996; Bakowski and Parekh, 2002; Kozak et al., 2002; Prakriya and Lewis, 2002), and the same is true for *Drosophila* CRAC channels (Fig. 7). From the measured reversal potential, *Drosophila* CRAC channels exhibited a Cs^+/Na^+ permeability ratio of ~0.08, similar to values of 0.09 and 0.13 observed previously for mammalian CRAC channels (Bakowski and Parekh, 2002; Prakriya and Lewis, 2002). The corresponding P_{Cs}/P_{Na} ratio for *C. elegans* SOC was ~0.6 (Estevez et al., 2003). Inward Cs^+ current through *Drosophila* CRAC channels was not detected, similar to the lack of inward Cs^+ current through mammalian CRAC channels (Lepple-Wienhues and Cahalan, 1996).

Single-channel Conductance and Estimated Number of Channels Per Cell

Another distinctive feature of the mammalian CRAC channel is its single-channel conductance, too small to be measured directly and estimated to be ~20 fS by measurement of variance and mean currents during current development (Zweifach and Lewis, 1993; Prakriya and Lewis, 2002). Noise analysis can significantly underestimate the single-channel conductance if the data are filtered excessively, or if the underlying assumption is incorrect that changes in mean current are caused by a change in P_o of a fixed total number of channels (Jackson and Strange, 1995), as for example in a homogeneous population of channels that have high open probability and activate by increasing the number of conducting channels. However, this latter possibility was tested and rejected in mammalian CRAC channels by evaluating monovalent current and variance in the presence and absence of 1 μM divalent to produce fast channel block (Prakriya and Lewis, 2002); rather than increasing noise, fast channel block decreased the variance to mean ratio, consistent with low P_o. With appropriate caveats in mind, we can proceed to a comparison of single-channel conductance values estimated by noise analysis and to a calculation of the number of channels in *Drosophila* S2 cells. The average unitary current of 6.9 fA corresponds to a single-channel conductance of 36 fS, compared with 21 fS for CRAC channels in Jurkat T cells under similar measurement conditions at −110 mV in 20 mM Ca^{2+}, in both cases assuming a reversal potential of 80 mV (Prakriya and Lewis, 2002). At the time of maximal current development, the number of conducting CRAC channels in S2 cells is ~10,000 per cell, obtained by dividing the peak macroscopic Ca^{2+} current (67 ± 10 pA, $n = 10$ cells) by the unitary Ca^{2+} current (6.9 fA). Considering that the open probability may be very low (<0.1), based upon the linear relationship of variance to mean current, the total number of channels N, calculated from $N = \bar{I} / (i P_o)$, is conservatively >100,000 per cell. Normalized for the cell surface area determined by measurement of whole-cell capacitance, this corresponds to a surface density of >71 channels/μM². For experiments with Ba^{2+}, the larger single-channel conductance value of 420 fS in 20 mM Ba^{2+} yields a calculated value of >23,000 channels per cell, a number that is likely to be underestimated since inactivation was not completely removed by the hyperpolarizing pulse during sustained exposure to Ba^{2+}. Even without correcting for a low P_o value, it appears that the CRAC channel is present at remarkably high levels in S2 cells. The current density averaged 3.3 pA/pF in 2 mM Ca^{2+} (Table II) and was doubled in 20 mM Ca^{2+}. In mammalian cells, estimates of CRAC current density measured in 10–20 mM external Ca^{2+} range from 0.5 to 2 pA/pF (Hoth and Penner, 1993; Zweifach and Lewis, 1993; Parekh et al., 1997b; Ehring et al., 2000; Prakriya and Lewis, 2002). Thus, the CRAC current density is 3- to 12-fold higher in S2 cells than in mammalian T cells, mast cells, or related cell lines.

Pharmacology

We tested three types of agents that have been shown to affect CRAC channels in mammalian cells. Lanthanum and gadolinium are known as effective CRAC channel antagonists in mammalian cells (Hoth and Penner, 1993; Ross and Cahalan, 1995). Gd^{3+} potently suppressed *Drosophila* CRAC current with an IC_{50} value of ~50 nM, similar to that observed in mouse thymocytes (Ross and Cahalan, 1995). La^{3+} (1 μM) also blocked the Ca^{2+} current completely, more potently than that reported for *C. elegans* I_{SOC} with an IC_{50} value of 9 μM (Estevez et al., 2003). SKF 96365 was originally reported to be an inhibitor of receptor-mediated Ca^{2+} entry (Merritt et al., 1990) and later shown to suppress

CRAC current (Chung et al., 1994). In S2 cells, the first application of SKF 96365 (20 μM) blocked the Ca^{2+} current almost completely, and this effect was partially reversible. The concentration at which SKF suppresses *Drosophila* CRAC currents is similar to that used to block I_{CRAC} in mast cells (Franzius et al., 1994), Jurkat T cells (Prakriya and Lewis, 2002), and RBL cells (Kozak et al., 2002). In contrast, SKF 96365 at even 100 μM did not abolish the *C. elegans* SOC current (Estevez et al., 2003). 2-APB was described initially as a blocker of the IP_3 receptor (Maruyama et al., 1997), and was later used to implicate a direct role of the IP_3 receptor in CRAC channel function (Ma et al., 2000). However, subsequent evidence showed that thapsigargin-evoked Ca^{2+} influx and CRAC channel currents could be blocked by 2-APB even in cells that lacked IP_3 receptors (Ma et al., 2001; Prakriya and Lewis, 2001). The dual effect of this drug on CRAC current in mammalian cells was thoroughly investigated in Jurkat T cells and RBL cells (Prakriya and Lewis, 2001). It is particularly striking that in S2 cells, just as in mammalian cells, 2-ABP potentiated CRAC currents at low concentrations (5–14 μM) and inhibited them at higher concentrations. In *C. elegans* epithelial cells, 100 μM 2-APB reversibly blocked I_{SOC} by ~90%, whereas 5 μM concentration did not have any significant effect (Estevez et al., 2003). We conclude that *Drosophila* CRAC channels in S2 cells exhibit pharmacological properties that are similar to those in mammalian CRAC channels.

Advantages for Future Studies

Many aspects of the CRAC channel remain mysterious, including the mechanism of activation and the gene (or genes) that encode the channel. In mammalian cells, TRP homologues remain as promising candidates to mediate SOC channel activity in various cell types. Leading recent contenders include TRPC1 (Mori et al., 2002), TRPC3 (Philipp et al., 2003), TRPC4 (Philipp et al., 2000), and TRPV6 (CaT1) (Voets et al., 2001; Yue et al., 2001; Cui et al., 2002; Schindl et al., 2002), but these identifications remain controversial and the issue has not yet been settled (Voets et al., 2001; Prakriya and Lewis, 2003). Other investigators have provided evidence implicating molecules not related to TRP in the regulation of functional SOC channels (Li et al., 2003; Ma et al., 2003). Here, we have presented evidence that the CRAC channel in S2 cells represents the *Drosophila* homologue of the mammalian CRAC channel, based on biophysical and pharmacological similarities. With the absence of contaminating currents from other channel types, S2 cells offer additional experimental advantages to investigate the molecular components and activation mechanisms of CRAC channels. The CRAC channel numbers per cell and surface density are higher in *Drosophila* S2 cells than previously reported in mammalian cells. Moreover, the *Drosophila* S2 cell culture system is ideally suited for gene silencing by RNA interference as a powerful tool to examine function, in that long, 500 base-pair (bp) double-stranded RNA probes are taken up easily from the medium by S2 cells (Worby et al., 2001). The use of 500 bp RNA probes increases the likelihood of producing an efficient small, interfering RNA (siRNA) and thereby reduces optimization steps in designing RNA probes for RNAi. These considerations enhance the feasibility of conducting a high-throughput RNAi-based screen in S2. Since the *Drosophila* genome is much smaller and better examined than the human genome, S2 cells provide the ideal model system to test the role of candidate genes in CRAC channel function by systematically suppressing functional expression by RNAi. Based on these properties, and the adaptability for FLIPR-based, higher-throughput, assays of Ca^{2+} signaling, S2 cells provide a useful system for molecular and functional characterization of CRAC channels and for identifying the mechanisms controlling activation of these channels.

We thank Dr. Lu Forrest and Dr. Olga Safrina for help with cell culture and Dr. J. Ashot Kozak for valuable comments on the manuscript.

This work was supported by a UC Star Biotech grant 01-10139 through the University of California and by grant #NS14609 from the National Institutes of Health.

David C. Gadsby served as editor.

Submitted: 20 November 2003
Accepted: 6 January 2004

REFERENCES

Almers, W., and E.W. McCleskey. 1984. Non-selective conductance in calcium channels of frog muscle: calcium selectivity in a single-file pore. *J. Physiol.* 353:585–608.

Bakowski, D., and A.B. Parekh. 2002. Monovalent cation permeability and Ca^{2+} block of the store-operated Ca^{2+} current I_{CRAC} in rat basophilic leukemia cells. *Pflugers Arch.* 443:892–902.

Christian, E.P., K.T. Spence, J.A. Togo, P.G. Dargis, and J. Patel. 1996. Calcium-dependent enhancement of depletion-activated calcium current in Jurkat T lymphocytes. *J. Membr. Biol.* 150:63–71.

Chung, S.C., T.V. McDonald, and P. Gardner. 1994. Inhibition by SK&F 96365 of Ca^{2+} current, IL-2 production and activation in T lymphocytes. *Br. J. Pharmacol.* 113:861–868.

Cordova, D., V.R. Delpech, D.B. Sattelle, and J.J. Rauh. 2003. Spatiotemporal calcium signaling in a *Drosophila melanogaster* cell line stably expressing a *Drosophila* muscarinic acetylcholine receptor. *Invert Neurosci.* 5:19–28

Cui, J., J.S. Bian, A. Kagan, and T.V. McDonald. 2002. CaT1 contributes to the stores-operated calcium current in Jurkat T-lymphocytes. *J. Biol. Chem.* 277:47175–47183.

Ehring, G.R., H.H. Kerschbaum, C.M. Fanger, C. Eder, H. Rauer, and M.D. Cahalan. 2000. Vanadate induces calcium signaling, Ca^{2+} release-activated Ca^{2+} channel activation, and gene expression in T lymphocytes and RBL-2H3 mast cells via thiol oxidation. *J. Immunol.* 164:679–687.

Estevez, A.Y., R.K. Roberts, and K. Strange. 2003. Identification of

store-independent and store-operated Ca^{2+} conductances in *Caenorhabditis elegans* intestinal epithelial cells. *J. Gen. Physiol.* 122: 207–223.

Fasolato, C., M. Hoth, and R. Penner. 1993. A GTP-dependent step in the activation mechanism of capacitative calcium influx. *J. Biol. Chem.* 268:20737–20740.

Feske, S., J. Giltnane, R. Dolmetsch, L.M. Staudt, and A. Rao. 2001. Gene regulation mediated by calcium signals in T lymphocytes. *Nat. Immunol.* 2:316–324.

Fierro, L., and A.B. Parekh. 2000. Substantial depletion of the intracellular Ca^{2+} stores is required for macroscopic activation of the Ca^{2+} release-activated Ca^{2+} current in rat basophilic leukaemia cells. *J. Physiol.* 522:247–257.

Franzius, D., M. Hoth, and R. Penner. 1994. Non-specific effects of calcium entry antagonists in mast cells. *Pflugers Arch.* 428:433–438.

Hamill, O.P., A. Marty, E. Neher, B. Sakmann, and F.J. Sigworth. 1981. Improved patch-clamp techniques for high-resolution current recording from cells and cell-free membrane patches. *Pflugers Arch.* 391:85–100.

Hardie, R.C., and B. Minke. 1992. The trp gene is essential for a light-activated Ca^{2+} channel in *Drosophila* photoreceptors. *Neuron.* 8:643–651.

Hardie, R.C., and B. Minke. 1995. Phosphoinositide-mediated phototransduction in *Drosophila* photoreceptors: the role of Ca^{2+} and trp. *Cell Calcium.* 18:256–274.

Hardie, R.C., and P. Raghu. 1998. Activation of heterologously expressed *Drosophila* TRPL channels: Ca^{2+} is not required and InsP3 is not sufficient. *Cell Calcium.* 24:153–163.

Hermosura, M.C., M.K. Monteilh-Zoller, A.M. Scharenberg, R. Penner, and A. Fleig. 2002. Dissociation of the store-operated calcium current I(CRAC) and the Mg-nucleotide-regulated metal ion current MagNuM. *J. Physiol.* 539:445–458.

Hess, P., and R.W. Tsien. 1984. Mechanism of ion permeation through calcium channels. *Nature.* 309:453–456.

Hoth, M. 1995. Calcium and barium permeation through calcium release-activated calcium (CRAC) channels. *Pflugers Arch.* 430: 315–322.

Hoth, M., and R. Penner. 1992. Depletion of intracellular calcium stores activates a calcium current in mast cells. *Nature.* 355:353–356.

Hoth, M., and R. Penner. 1993. Calcium release-activated calcium current in rat mast cells. *J. Physiol.* 465:359–386.

Jackson, P.S., and K. Strange. 1995. Single-channel properties of a volume-sensitive anion conductance. Current activation occurs by abrupt switching of closed channels to an open state. *J. Gen. Physiol.* 105:643–660.

Kozak, J.A., H.H. Kerschbaum, and M.D. Cahalan. 2002. Distinct properties of CRAC and MIC channels in RBL cells. *J. Gen. Physiol.* 120:221–235.

Lepple-Wienhues, A., and M.D. Cahalan. 1996. Conductance and permeation of monovalent cations through depletion-activated Ca^{2+} channels (I_{CRAC}) in Jurkat T cells. *Biophys. J.* 71:787–794.

Lewis, R.S. 2001. Calcium signaling mechanisms in T lymphocytes. *Annu. Rev. Immunol.* 19:497–521.

Lewis, R.S., and M.D. Cahalan. 1989. Mitogen-induced oscillations of cytosolic Ca^{2+} and transmembrane Ca^{2+} current in human leukemic T cells. *Cell Regul.* 1:99–112.

Li, H., L.M. Ayer, J. Lytton, and J.P. Deans. 2003. Store-operated cation entry mediated by CD20 in membrane rafts. *J. Biol. Chem.* 278:42427–42434.

Ma, H.T., R.L. Patterson, D.B. van Rossum, L. Birnbaumer, K. Mikoshiba, and D.L. Gill. 2000. Requirement of the inositol trisphosphate receptor for activation of store-operated Ca^{2+} channels. *Science.* 287:1647–1651.

Ma, H.T., K. Venkatachalam, H.S. Li, C. Montell, T. Kurosaki, R.L. Patterson, and D.L. Gill. 2001. Assessment of the role of the inositol 1,4,5-trisphosphate receptor in the activation of transient receptor potential channels and store-operated Ca^{2+} entry channels. *J. Biol. Chem.* 276:18888–18896.

Ma, R., D. Rundle, J. Jacks, M. Koch, T. Downs, and L. Tsiokas. 2003. Inhibitor of myogenic family: A novel suppressor of store-operated currents through an interaction with TRPC1. *J. Biol. Chem.* 278:52763–52772.

Maruyama, T., T. Kanaji, S. Nakade, T. Kanno, and K. Mikoshiba. 1997. 2APB, 2-aminoethoxydiphenyl borate, a membrane-penetrable modulator of Ins(1,4,5)P_3-induced Ca^{2+} release. *J. Biochem. (Tokyo).* 122:498–505.

Merritt, J.E., W.P. Armstrong, C.D. Benham, T.J. Hallam, R. Jacob, A. Jaxa-Chamiec, B.K. Leigh, S.A. McCarthy, K.E. Moores, and T.J. Rink. 1990. SK&F 96365, a novel inhibitor of receptor-mediated calcium entry. *Biochem. J.* 271:515–522.

Minke, B., and K. Agam. 2003. TRP gating is linked to the metabolic state and maintenance of the *Drosophila* photoreceptor cells. *Cell Calcium.* 33:395–408.

Minke, B., and B. Cook. 2002. TRP channel proteins and signal transduction. *Physiol. Rev.* 82:429–472.

Minke, B., C. Wu, and W.L. Pak. 1975. Induction of photoreceptor voltage noise in the dark in *Drosophila* mutant. *Nature.* 258:84–87.

Montell, C. 2003. The venerable inveterate invertebrate TRP channels. *Cell Calcium.* 33:409–417.

Montell, C., L. Birnbaumer, and V. Flockerzi. 2002. The TRP channels, a remarkably functional family. *Cell.* 108:595–598.

Montell, C., and G.M. Rubin. 1989. Molecular characterization of the *Drosophila* trp locus: a putative integral membrane protein required for phototransduction. *Neuron.* 2:1313–1323.

Mori, Y., M. Wakamori, T. Miyakawa, M. Hermosura, Y. Hara, M. Nishida, K. Hirose, A. Mizushima, M. Kurosaki, E. Mori, et al. 2002. Transient receptor potential 1 regulates capacitative Ca^{2+} entry and Ca^{2+} release from endoplasmic reticulum in B lymphocytes. *J. Exp. Med.* 195:673–681.

Parekh, A.B., A. Fleig, and R. Penner. 1997a. The store-operated calcium current I(CRAC): nonlinear activation by InsP3 and dissociation from calcium release. *Cell.* 89:973–980.

Parekh, A.B., A. Fleig, and R. Penner. 1997b. The store-operated calcium current I_{CRAC}: nonlinear activation by $InsP_3$ and dissociation from calcium release. *Cell.* 89:973–980.

Parekh, A.B., and R. Penner. 1997. Store depletion and calcium influx. *Physiol. Rev.* 77:901–930.

Philipp, S., B. Strauss, D. Hirnet, U. Wissenbach, L. Mery, V. Flockerzi, and M. Hoth. 2003. TRPC3 mediates T-cell receptor-dependent calcium entry in human T-lymphocytes. *J. Biol. Chem.* 278: 26629–26638.

Philipp, S., C. Trost, J. Warnat, J. Rautmann, N. Himmerkus, G. Schroth, O. Kretz, W. Nastainczyk, A. Cavalie, M. Hoth, and V. Flockerzi. 2000. TRP4 (CCE1) protein is part of native calcium release-activated Ca^{2+}-like channels in adrenal cells. *J. Biol. Chem.* 275:23965–23972.

Prakriya, M., and R.S. Lewis. 2001. Potentiation and inhibition of Ca^{2+} release-activated Ca^{2+} channels by 2-aminoethyldiphenyl borate (2-APB) occurs independently of IP_3 receptors. *J. Physiol.* 536:3–19.

Prakriya, M., and R.S. Lewis. 2002. Separation and characterization of currents through store-operated CRAC channels and Mg^{2+}-inhibited cation (MIC) channels. *J. Gen. Physiol.* 119:487–507.

Prakriya, M., and R.S. Lewis. 2003. CRAC channels: activation, permeation, and the search for a molecular identity. *Cell Calcium.* 33: 311–321.

Premack, B.A., T.V. McDonald, and P. Gardner. 1994. Activation of

Ca^{2+} current in Jurkat T cells following the depletion of Ca^{2+} stores by microsomal Ca^{2+}-ATPase inhibitors. *J. Immunol.* 152: 5226–5240.

Ramet, M., P. Manfruelli, A. Pearson, B. Mathey-Prevot, and R.A. Ezekowitz. 2002. Functional genomic analysis of phagocytosis and identification of a *Drosophila* receptor for E. coli. *Nature.* 416: 644–648.

Ross, P.E., and M.D. Cahalan. 1995. Ca^{2+} influx pathways mediated by swelling or stores depletion in mouse thymocytes. *J. Gen. Physiol.* 106:415–444.

Schindl, R., H. Kahr, I. Graz, K. Groschner, and C. Romanin. 2002. Store depletion-activated CaT1 currents in rat basophilic leukemia mast cells are inhibited by 2-aminoethoxydiphenyl borate. Evidence for a regulatory component that controls activation of both CaT1 and CRAC (Ca^{2+} release-activated Ca^{2+} channel) channels. *J. Biol. Chem.* 277:26950–26958.

Schneider, I. 1972. Cell lines derived from late embryonic stages of *Drosophila melanogaster. J. Embryol. Exp. Morphol.* 27:353–365.

Swatton, J.E., S.A. Morris, F. Wissing, and C.W. Taylor. 2001. Functional properties of *Drosophila* inositol trisphosphate receptors. *Biochem. J.* 359:435–441.

Towers, P.R., and D.B. Sattelle. 2002. A *Drosophila melanogaster* cell line (S2) facilitates post-genome functional analysis of receptors and ion channels. *Bioessays.* 24:1066–1073.

Voets, T., J. Prenen, A. Fleig, R. Vennekens, H. Watanabe, J.G. Hoenderop, R.J. Bindels, G. Droogmans, R. Penner, and B. Nilius. 2001. CaT1 and the calcium release-activated calcium channel manifest distinct pore properties. *J. Biol. Chem.* 276:47767–47770.

Worby, C.A., N. Simonson-Leff, and J.E. Dixon. 2001. RNA interference of gene expression (RNAi) in cultured *Drosophila* cells. *Sci STKE.* 2001:PL1.

Yagodin, S., R.C. Hardie, S.J. Lansdell, N.S. Millar, W.T. Mason, and D.B. Sattelle. 1998. Thapsigargin and receptor-mediated activation of *Drosophila* TRPL channels stably expressed in a *Drosophila* S2 cell line. *Cell Calcium.* 23:219–228.

Yagodin, S., N.B. Pivovarova, S.B. Andrews, and D.B. Sattelle. 1999. Functional characterization of thapsigargin and agonist-insensitive acidic Ca^{2+} stores in *Drosophila melanogaster* S2 cell lines. *Cell Calcium.* 25:429–438.

Yue, L., J.B. Peng, M.A. Hediger, and D.E. Clapham. 2001. CaT1 manifests the pore properties of the calcium-release-activated calcium channel. *Nature.* 410:705–709.

Zweifach, A., and R.S. Lewis. 1993. Mitogen-regulated Ca^{2+} current of T lymphocytes is activated by depletion of intracellular Ca^{2+} stores. *Proc. Natl. Acad. Sci. USA.* 90:6295–6299.

Zweifach, A., and R.S. Lewis. 1995a. Rapid inactivation of depletion-activated calcium current (ICRAC) due to local calcium feedback. *J. Gen. Physiol.* 105:209–226.

Zweifach, A., and R.S. Lewis. 1995b. Slow calcium-dependent inactivation of depletion-activated calcium current. Store-dependent and -independent mechanisms. *J. Biol. Chem.* 270:14445–14451.

Zweifach, A., and R.S. Lewis. 1996. Calcium-dependent potentiation of store-operated calcium channels in T lymphocytes. *J. Gen. Physiol.* 107:597–610.